View metadata, citation and similar papers at core.ac.uk
brought to you by CORE
provided by Publications of the IAS Fellows

New Journal of Physics
The open-access journal for physics

Structure–conductivity correlation in ferric chloride-doped poly(3-hexylthiophene)

Rajiv K Singh[1], Jitendra Kumar[1], Ramadhar Singh[1,3], Rama Kant[2], R C Rastogi[2], Suresh Chand[1] and Vikram Kumar[1]

[1] National Physical Laboratory, Dr. K.S. Krishnan Marg, New Delhi 110012, India
[2] Department of Chemistry, University of Delhi, Delhi 110007, India
E-mail: ramadhar@mail.nplindia.ernet.in

New Journal of Physics **8** (2006) 112
Received 14 May 2006
Published 5 July 2006
Online at http://www.njp.org/
doi:10.1088/1367-2630/8/7/112

Abstract. Poly(3-hexylthiophene) (P3HT) matrix has been chemically doped (redox doping) by ferric chloride ($FeCl_3$) with different molar concentrations to get P3HT–$FeCl_3$ charge-transfer complexes. The effect of redox doping on photo-physical, structural, and morphological properties and dc electrical conductivity of P3HT matrices has been examined. The dc conductivity has been measured on films of pristine P3HT and P3HT–$FeCl_3$ charge-transfer complexes in the temperature range 6–300 K. Analysis of dc conductivity data reveals that in the temperature range 40–300 K, the dc conductivity is predominantly governed by Mott's 3-dimensional variable range hopping (3D-VRH); however, below 40 K tunnelling seems to dominate. A slight deviation from 3D-VRH to 1D-VRH is observed with an increase in doping level or precisely with an increase in the extent of P3HT–$FeCl_3$ charge-transfer complexes. We attribute this deviation to the induced expansion in crystallographic lattices as revealed by x-ray diffraction data and formation of discrete conducting domains as observed by atomic force microscope imaging.

[3] Author to whom any correspondence should be addressed.

PII: S1367-2630(06)24510-5
© IOP Publishing Ltd and Deutsche Physikalische Gesellschaft

Contents

1. Introduction

Extensive research in the field of conducting polymers started in 1977 when it was demonstrated that polyacetylene, the simplest conjugated polymer, can be made electrically conductive through a chemical doping (redox doping) reaction which involves partial reduction or oxidation (n-type or p-type doping) of its spatially extended π-bonding system [1, 2]. This discovery induced intensive research in this area especially devoted to the synthesis, doping, spectroscopic, photophysical, structural and electrical characterization of these systems such as polyacetylene, polypyrrole, polyaniline, polythiophene, polyparaphenylene and their copolymers, composites or blends, etc. These conjugated polymers find widespread technological applications in electronic and display devices such as in batteries, super capacitors, electromagnetic interference shielding, biological and microbial sensors, field effect transistors, solar cells, organic light emitting diodes, etc [3]–[16]. They also offer a unique combination of properties that make them suitable alternatives for different inorganic semi-conducting materials currently being used in microelectronics. Among all these conjugated polymers, polythiophenes are attracting the immense interest of researchers because of their good environmental stability, easy processability and easy modification of the properties by varying the synthesis parameters [17, 18]. Poly(3-alkylthiophenes) are soluble in common organic solvents as well as melt processable, having excellent electronic and optical properties suitable for various device applications. They can be synthesized by both electrochemical and chemical polymerization techniques; however, the polymers prepared by electrochemical route are not solution processable. In the chemical polymerization technique, synthesis of processable polymers requires oxidation of the monomer with an oxidant such as ferric chloride and optimization of different synthesis parameters used for polymerization [17, 18]. However, before these materials are used for device applications, it is important to understand the formation of charge carriers and transport of carriers through matrices of doped conducting polymers.

As regards the nature of charge formation in conjugated polymers, the highly mobile charge-carrying species in the polyacetylene chain have been modelled as solitons [19]. However, the non-degenerate ground states preclude the existence of solitons in other conjugated polymers [20]. Many electron spin resonance and optical studies on polyheterocyclics such as polypyrroles and polythiophenes have been reported [18], [21]–[29] which indicates that the charge carriers in these systems are polarons or bipolarons. Still, it is not conclusively established that the charge carriers are polarons or bipolarons. Generally, it is believed that the polarons are formed at lower doping concentration, which get combined to form bipolarons at higher doping concentration. Furthermore, several studies [18], [30]–[54] have been reported to understand the mechanism of dc electrical conduction in these conjugated polymers. However, the basic charge-transport mechanism in these systems is not conclusively established as yet because the prime interest of the researcher was centred on achieving high electrical conductivity by doping.

Several models [30]–[32], [35, 38, 46, 51, 52, 54] have been proposed to explain the conduction mechanism in these materials similar to the models developed for amorphous semiconductors [55]. During the last 2–3 decades, some of these models have been used to explain the observed experimental dc conductivity data of conjugated polymers; however, lack of long range ordering in most of the conjugated polymeric systems does not allow one to explain the mechanism of conduction completely. This is due to the fact that different polymeric systems contain different types of electronic and structural defects. Kivelson [32] was the first to propose a model in which the charge transport occurs by hopping between neutral and charged soliton states at iso-energetic levels. This model was modified [46] for materials which have non-degenerate ground state having inter-polaronic hopping conduction. The other models widely used to explain the dc conductivity data of conjugated polymers are fluctuation induced tunnelling (FIT) [42] and Mott's variable range hopping (VRH) [55]. The FIT model was proposed [42] for a granular system in which tiny conducting domains formed during doping participate in the delocalization of charge carriers by tunnelling between the conducting metallic islands. The macroscopic conductivity in most of the conjugated polymers is assumed to result from the hopping process except in ordered polyacetylene and some forms of polyaniline. In the hopping conduction process, each state can have only one charge carrier for each spin direction. In the case of strong localization, the charge carrier will hop to a nearest-neighbouring state and the hopping conductivity will be proportional to Boltzmann's factor $\exp(-W/k_{\mathrm{B}}T)$, where W is the difference of energy between two states and is called the hopping energy or activation energy required for a charge carrier to hop from one site to another. However, when charge carriers are not strongly localized, a charge carrier can jump to the sites for which the activation energy is small and can reside further away; then the transport occurs by VRH [55]. It is worthwhile to mention here that Mott's VRH model [55] has been extensively used to explain the mechanism of charge transport in many conjugated polymeric systems such as doped polyacetylenes [45], polypyrrole [39, 40, 56, 57], polyaniline [37] and its composites [48], microtubules of polyaniline and polypyrrole [58], poly (3-methylthiophene) [59], poly (3-octylthiophene) [60], etc. Recently, the VRH as possible origin of a universal relation between conductivity and mobility in a disordered organic semiconductor [51] and VRH in low-dimensional polymer structures [52] have been reported.

In the last two decades, poly(3-alkylthiophenes) have been extensively investigated for its structural [61]–[69], optical [70]–[73], and morphological [74]–[78] and electrical properties [43, 59, 60, 77]; however, no details are available in the literature regarding the effect of doping level on these properties and a correlation between them. In the present paper, we report our detailed investigation of the effect of doping level on photo-physical, structural, morphological

and electrical properties of pristine and lightly doped poly(3-hexylthiophene) (P3HT) films. For the first time, we have tried to correlate the doping induced structural, optical, and morphological changes with the changes in electrical conductivity of progressively doped (oxidized) P3HT films. The measured dc conductivity data in the temperature range 6–300 K have been analysed by using different theoretical models (as described in previous paragraph) and are reported in the present paper.

2. Experimental details

2.1. Synthesis and purification of P3HT

For the present investigation, a good quality P3HT polymer was synthesized by chemical oxidative polymerization at low temperature (258 K) [75, 78, 79]. Drop-wise addition of 3-hexylthiophene monomer (0.1 M) into ferric chloride ($FeCl_3$) suspension (0.4 M) in chloroform ($CHCl_3$) kept at 258 K in an inert atmosphere for over 12 h, results into a high quality P3HT polymer. Synthesized P3HT was precipitated from reaction mixture by adding copious amount of methanol. Repeated purification was performed by methanol and de-ionized water to remove methanol soluble oligomers and excess of oxidant impurity. The pristine P3HT polymer was obtained after removing the intercalated oxidant impurity from polymer matrix by repeated treatment with liquid ammonia (NH_3) and ethylenediaminetetraacetic acid (EDTA) [78]–[80]. Then the solution of pristine P3HT, prepared in chloroform, was casted on quartz plate at room temperature. A smooth film (thickness $\sim$15 μm) free from any pin holes, having good mechanical strength, was obtained and subsequently used for doping and related measurements.

2.2. Redox doping of P3HT by $FeCl_3$

Since the conjugated polymers in their pristine form do not contain intrinsic charge carriers, therefore they must be provided extrinsically and can be achieved by a charge-transfer process, generally called doping. For the present investigation, doping of P3HT (a weak base) has been accomplished by using $FeCl_3$ (a weak acid, oxidant) involving electron exchange (redox reaction) between the two. Nine pieces of the P3HT film were cut and dipped separately into different concentrations of $FeCl_3$ (0.001–1 M) in nitromethane (CH_3NO_2) solution for 12 h. Then the $FeCl_3$-doped P3HT films were repeatedly washed with methanol and dried under nitrogen gas for several minutes and preserved in vacuum. Four thin films (thickness $\sim$1 μm) were prepared by solution casting of chloroform solution of P3HT polymer on quartz substrate at room temperature, from which three films were doped in a similar way as the free standing films (thickness $\sim$15 μm), by taking the different strength of doping solution of $FeCl_3$ (0.001, 0.125 and 0.250 M) in CH_3NO_2 for 12 h. The details of the doping procedure were described in our previous work [60].

2.3. Measurements

Fourier transform infrared (FT-IR) spectra of pristine and doped P3HT films were recorded on a PerkinElmer FT-IR Spectrometer in the range 4000–400 cm^{-1}. The changes in optical absorptions of pristine and doped thin P3HT films (thickness $\sim$1 μm), grown on quartz substrate, were probed

by recording ultraviolet–visible (UV–Vis) spectra on Shmandzli 2401 PC Spectrophotometer. The changes in crystallographic parameters upon progressive doping, were obtained by D-8 Advanced X-ray Diffractometer (Bruker), and were characterized by different numbers of strong and narrow peaks for CuK_α ($\lambda = 1.5404$ Å) radiation in their x-ray diffraction patterns. The 3-dimensional (3D) topography of pristine and doped P3HT films (thickness $\sim$1 μm) was obtained by a Pacific Nanotechnology (Nano-R^{TM}) atomic force microscope (AFM). For dc conductivity measurement, gold electrodes were vacuum ($\sim 10^{-6}$ Torr) evaporated on both sides of these P3HT films (thickness $\sim$15 μm), thus making an Au/P3HT/Au sandwich structure. For this, these films were masked in such a way (as shown in inset of figure 5) that gold could be deposited on both sides (transverse sides) of the P3HT films sandwiching a common area of $3.14 \times 0.25 \times 0.25\,cm^2$ and the two gold strips, one from each transverse side extends beyond the common sandwiched area. The extended gold strips of both sides were used to make electrical contacts with the help of electrically conducting silver paste and copper wire, thus ruling out any possibility of short circuiting [60].

All the samples used in the present investigation have been marked in figure 5 as HT0 (pristine) and HT1 to HT9 (doped). The room temperature dc conductivity of these samples varies between $2.61 \times 10^{-7}\,S\,cm^{-1}$ (HT0) and $2.76 \times 10^{-3}\,S\,cm^{-1}$ (HT9). The temperature dependence of dc conductivity of these pristine and doped P3HT films (thickness $\sim$15 μm) was measured in a closed cycle helium cryostat (ARS, USA) with Lakeshore 331 temperature controller in the range 6–300 K by using Keithley's 238 Source Meter and 480 Picoammeter.

3. Results and discussion

One of the most challenging tasks regarding conducting polymers has been the understanding of charge formation and its transport through π-conjugated rigid wire. To better understand the above-mentioned aspects of conducting polymers, we have closely monitored the effect of electron transfer from the π-conjugated backbone of P3HT to an electron acceptor ($FeCl_3$-oxidant) on the various inherent bond vibrations (stretching, deformation, rocking, etc) upon IR excitation (figure 1) and on the changes in electronic transitions (figure 2) due to UV–Vis excitation on progressively doped P3HT–$FeCl_3$ redox matrices. Furthermore, from x-ray diffraction data (XRD), we have tried to show the physical approach of dopant ions ($FeCl_4^-$) to an electron rich π-conjugated backbone of P3HT in order to receive an electron from the latter and its consequence on expansion of π–π stacks, as is evident from figure 3. Moreover, this gives an idea of region specific doping and evolution of fairly homogeneous doping regions (more precisely conducting regions) (figure 3), which controls the macroscopic conducting behaviour of the present system (described in later part of this paper). Before going into the details of all these spectroscopic and morphological characterization, it seems imperative to mention and sketch here the visualized doping phenomenon as illustrated in our previous study [60]. The idea of including this scheme again (which was previously for a single doping concentration), though in modified form (includes XRD data exhibiting expansion in π–π stacks), is that it will help in understanding the present work related with a range of doping concentration more clearly. This is schematically represented in scheme 1.

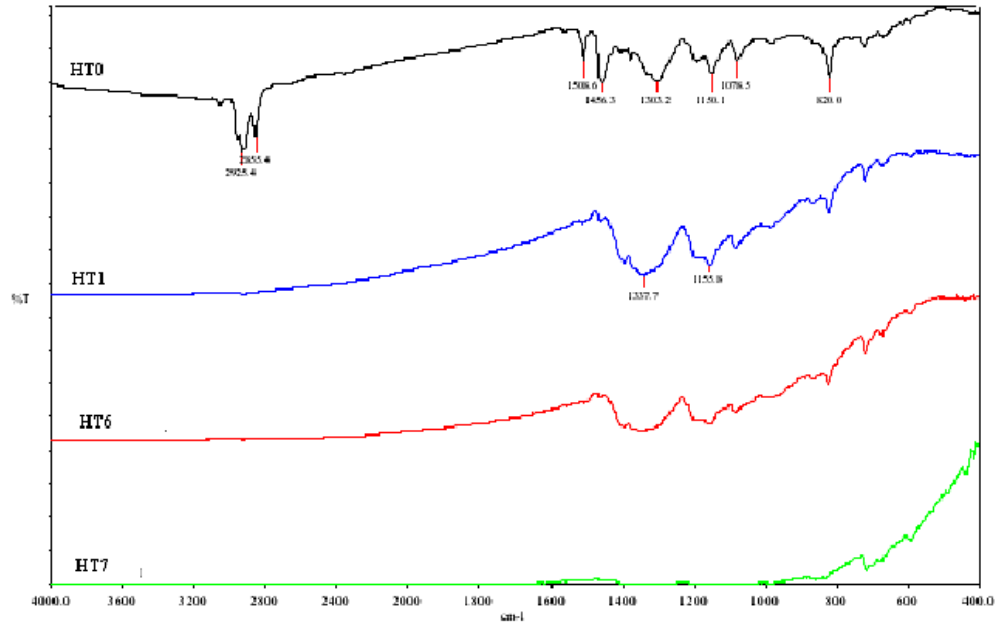

Figure 1. The characteristic FT-IR bands: (a) pristine P3HT (HT0), (b) 0.001 M $FeCl_3$-doped P3HT (HT1), (c) 0.125 M $FeCl_3$-doped P3HT (HT6), and (d) 0.250 M $FeCl_3$-doped P3HT (HT7).

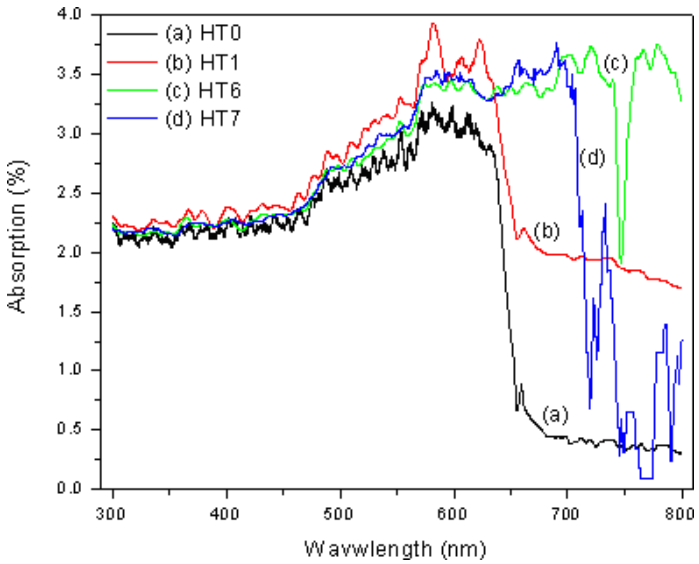

Figure 2. UV–Vis absorption maximas and absorption edges: (a) pristine P3HT (HT0), (b) 0.001 M $FeCl_3$-doped P3HT (HT1), (c) 0.125 M $FeCl_3$-doped P3HT (HT6), and (d) 0.250 M $FeCl_3$-doped P3HT (HT7).

3.1. FT-IR investigations

The changes in FT-IR spectra, induced by dopants through formation of increasing number of P3HT–$FeCl_3$ charge-transfer complexes are shown in figure 1. The details of different

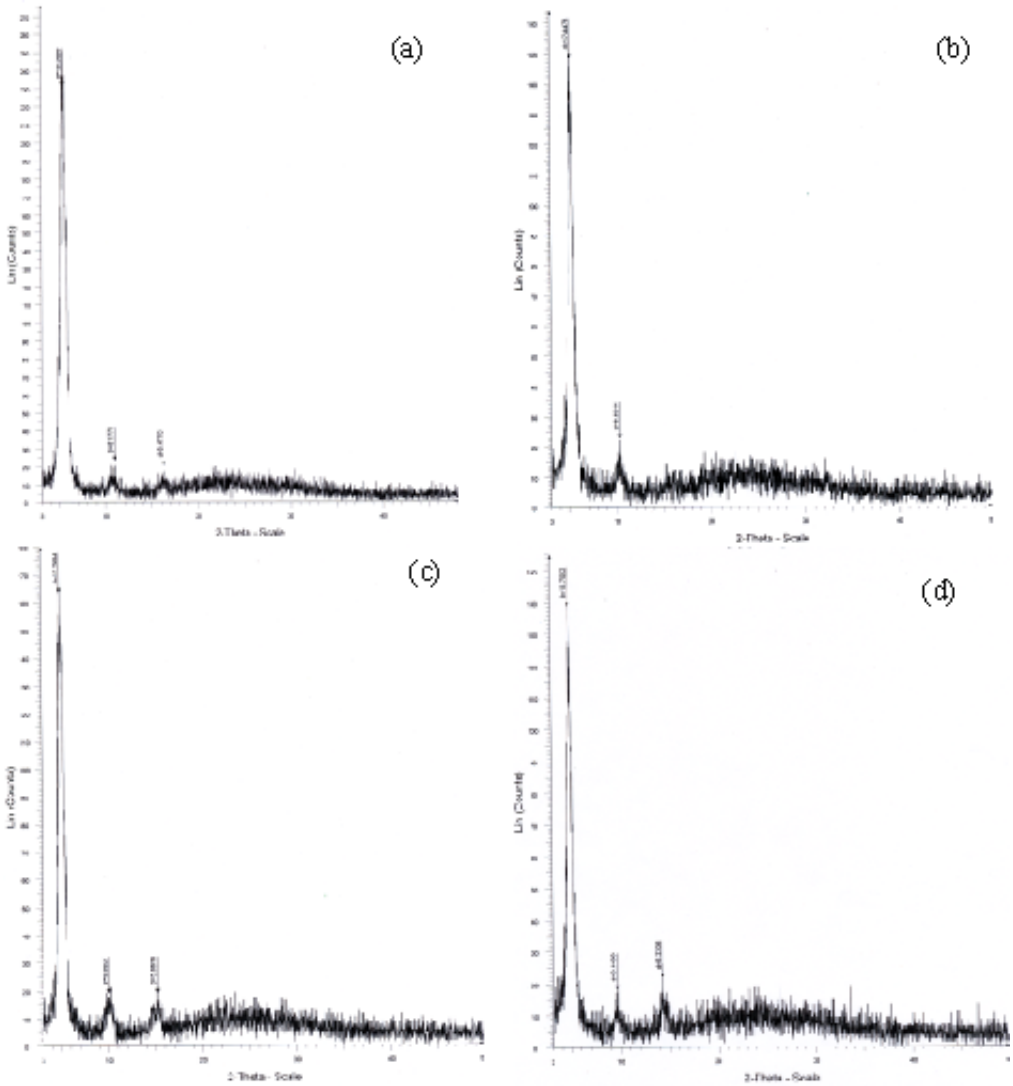

Figure 3. XRD diffraction patterns obtained for pristine and $FeCl_3$-doped P3HT films ($\sim$1 μm): (a) pristine P3HT (HT0), (b) 0.001 M $FeCl_3$-doped P3HT (HT1), (c) 0.125 M $FeCl_3$-doped P3HT (HT6), and (d) 0.250 M $FeCl_3$-doped P3HT (HT7).

IR bands for pristine poly(3-octylthiophene) (P3OT) was described in our recent work [78]. It is important to mention here that the FT-IR spectra pass through a series of changes in successively doped samples by increasing amount of dopant concentration (figure 1). Some important changes are: loss of bands in the region 3100–2855 cm^{-1}, i.e. the characteristic stretching vibrational bands due to aromatic hydrogen ($\sim$3100 cm^{-1}) and alkyl hydrogen ($\sim$2950–2850 cm^{-1}), respectively. Low to high losses in the middle spectral region (1500–1300 cm^{-1}) and loss of bands in the lower spectral region which is the characteristic of pristine polymer and the characteristic band arises due to P3HT–$FeCl_3$ charge-transfer complexes ($\sim$970 cm^{-1}) and a broad band beyond 800–400 cm^{-1} are also seen.

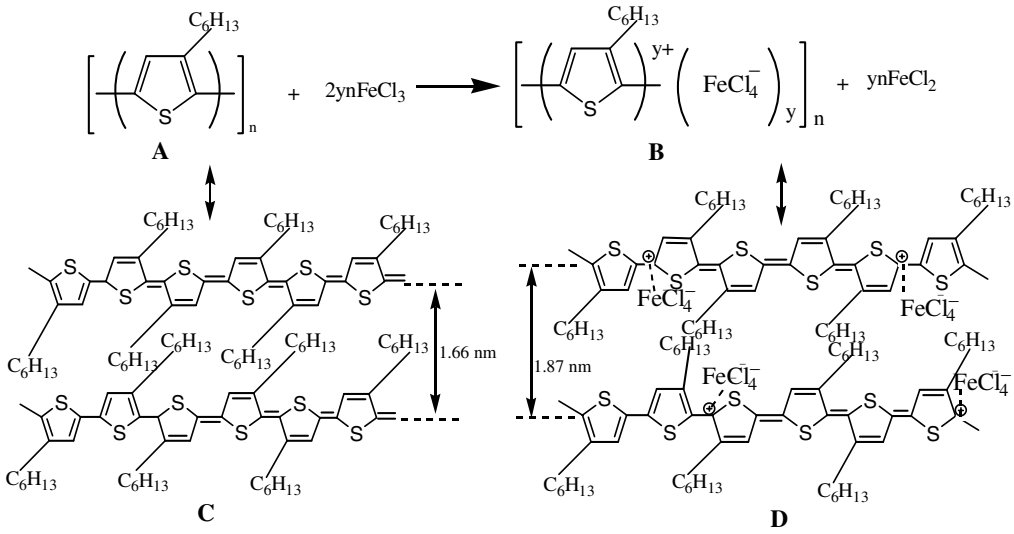

Scheme 1. A is the molecular formula of P3HT polymer and B represents the P3HT-reduced ferric chloride ($FeCl_4^-$) charge-transfer complex. Drawing C represents the distance between π–π stacks when polymer is in pristine form, whereas drawing D represents distance between π–π stacks in their complex form. The expansion in π–π stacks from 1.66 nm (C) to 1.87 nm (D) after intercalation of dopant species ($FeCl_4^-$) to polymeric chains has been calculated from XRD data.

3.2. UV–Vis spectroscopy

The UV–Vis spectra witness a marked change in its π–π^* transition [70] (figures 2(a)–(d)), from intense sharp peaks ($\lambda_{max} = 510$ nm) i.e. characteristics of pristine P3HT (figure 2(a)) through a slightly broader peak for very lightly doped (0.001 M $FeCl_3$) film (figure 2(b)) to significantly broader peaks for moderately doped (0.125 and 0.250 M $FeCl_3$) films (figures 2(c) and (d)). Other notable changes observed are in the absorption edges of pristine and very lightly doped samples showing distinct absorption edges corresponding to highly delocalized electron rich π-conjugated backbone of pristine P3HT and formation of few charges along the π-conjugated backbone for very lightly doped P3HT, whereas no sharp absorptions are seen in the case of moderately doped matrices (figures 2(c) and (d)) corresponding to the sharp reduction in electron density along π-conjugated backbone and hence formation of more and more charge-transfer sites [17, 81].

3.3. XRD studies

XRD patterns obtained for one pristine and three $FeCl_3$-doped samples of P3HT solid thin films (2θ values ranging from 3 to 50), exhibiting structural properties typically of homogeneous and quasi-crystalline polythiophenes and expansion in crystallites lattice spacing upon insertion of dopant ions in between π–π stacks, are shown in figure 3. The d-values of these samples are summarized in table 1. It can be seen from figures 3(a)–(d) and table 1 that there is a systematic increase in d-values with increase in doping concentration because more and more dopant ions get inserted and intercalated in between π–π stacks. It is significant to note that the crystalline nature [61] exists even in doped P3HT matrices as the shape of XRD peaks for

Table 1. Summary of changes in the spacing of π–π stacks (d-values) upon intercalation of dopant ions with π-conjugated chains in pristine and $FeCl_3$-doped P3HT films.

Sample	d_1 (Å)	d_2 (Å)	d_3 (Å)
HT0 (pristine)	16.5999	8.1771	5.4770
HT1 (0.001 M)	17.4478	8.6341	—
HT6 (0.125 M)	17.7684	8.8837	5.8616
HT7 (0.250 M)	18.7012	9.1939	6.2208

various doping levels (figures 3(b)–(d)) are almost same as that of pristine P3HT (figure 3(a)). Another significant change is an increase in d-spacing from 16.5999 to 18.7012 Å, showing slight expansion in π–π stacks which may cause lowering in the inter-chain interaction leading to lower crystallite dimensionality. The lowering of crystallite dimensionality in doped state may alter mode of charge carrier transport as compared to the mode of charge transport in pristine P3HT. It is significant to note here that two positively charged polymeric chains are electrostatically connected with negatively charged dopant species as shown in scheme 1. So even though π–π stacks expand slightly which might reduce inter-chain (π–π stacks) interaction and charge transport, the presence of a coulombic interaction between positively charged polymeric chains and negatively charged dopant species counterbalances it. This type of oppositely charged system in which positively charged polymeric chains are being interlinked electrostatically via negatively charged dopant species helps in maintaining the 3D inter-chain charge flowing path (scheme 1), as also revealed from the study of temperature-dependent dc conductivity discussed later in this paper.

3.4. AFM imaging

Figure 4 helps in understanding the hetero-structural (amorphous and crystalline) compositions of pristine P3HT matrix as well as specific regions of doping and thus giving an idea about conducting domains, namely their size and distribution. It is interesting to note the morphology displayed by pristine P3HT solid thin film ($\sim$1 μm) traced by AFM tips in demographic or tapping mode (figure 4(a)). The topographic changes obtained in tapping mode operation are attributed to the heterogeneity of the system under investigation in terms of its soft and hard regions. Figure 4(a) shows so many bright features in topographic image of pristine P3HT matrix, when pristine P3HT film was scanned by AFM in tapping mode. These bright features may correspond to the hard regions of P3HT matrix. We attribute these hard regions to the polymer crystallites, which consist of closely packed (π–π stacks) chains (scheme 1(c)) and area between these spikes to the amorphous part, which is without proper chain stacking. This result is supplemented by the results of XRD studies (figure 3(a)), which shows sharp peaks attributed to crystalline parts consisting of closely packed π–π stacks of P3HT matrix. Further, the line diagrams (figure 4(b)) showing low root mean square (rms) roughness values indicate that the structural features (amorphous and crystalline) are fairly homogeneous. Figure 4(c) is 3D topography of pristine P3HT matrix showing largely smooth surface taken by AFM in non-contact mode. The nature of the surface shown in figure 4(c) helps in understanding the progressive morphological evolution upon increasing extent of doping and hence gives idea

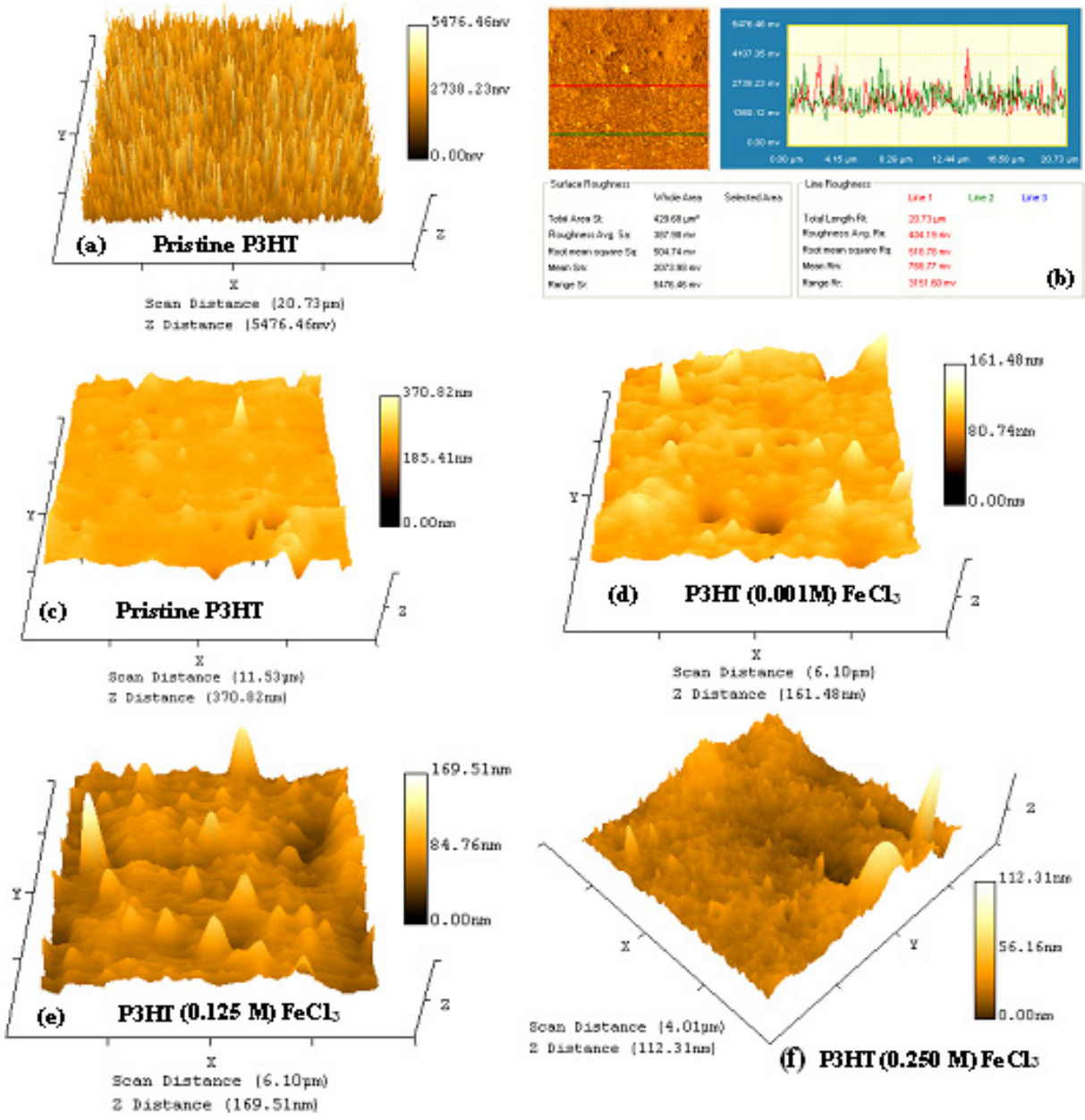

Figure 4. AFM 3D topography of pristine and doped P3HT solid thin films (∼1 μm): (a) topographs of pristine P3HT taken AFM operated in tapping mode, (b) surface roughness of pristine P3HT illustrated by AFM operated in tapping mode, and surface topographs: (c) pristine P3HT taken in non-contact mode (HT0) (d) 0.001 M $FeCl_3$-doped P3HT (HT1), (e) 0.125 M $FeCl_3$-doped P3HT (HT6), and (f) 0.250 M $FeCl_3$-doped P3HT (HT7).

about formation of conducting domains (regions where dopant species lie) in P3HT–$FeCl_3$ charge-transfer matrices. It is important to note here that the surface topograph of pristine P3HT film shows only a few bright regions, which makes the resultant surface roughness too high (up to ∼370 nm). Figures 4(d)–(f) show an increase in the number of conducting domains as well

as the increase in its homogeneous distribution as the extent of doping or formation of charge-transfer complex increases. The regions (in doped P3HT matrices) having dopant molecules will be hard (less elastic) as compared to regions having no dopant molecules (more elastic) [60]. Thus conducting domains are represented by bright regions in the topographic image shown in figures 4(d)–(f). Figure 4(d) shows the topographic image of only very lightly doped (0.001 M $FeCl_3$) P3HT–$FeCl_3$ charge-transfer complex, having low number of bright regions corresponding to the doped regions as compared to the topographic image of pristine P3HT (figure 4(c)). As the extent of doping increases to 0.125 M $FeCl_3$, the number of conducting domains increases (figure 4(e)), and for a moderately doped (0.250 M $FeCl_3$) P3HT film, not only does the number of conducting domains (bright regions) increase but the homogeneity of conducting domains distribution also increases significantly (figure 4(f)). The increase in number of fairly homogenously distributed conducting domains is attributed to the significant increase in conductivity of P3HT–$FeCl_3$ matrices.

3.5. Doping dependence of dc conductivity

Figure 5 shows the variation of dc conductivity (σ_{dc}) of different samples of P3HT as a function of $FeCl_3$ dopant concentration at room temperature (~300 K). The maximum conductivity $\sim 2.76 \times 10^{-3}\,S\,cm^{-1}$ is obtained for the sample (HT-9) having dopant concentration of 1 M. It is evident from figure 5 that the dependence of dc conductivity on dopant concentration indicates that the macroscopic conductivity initially increases up to a doping level of 0.025 M and thereafter the increase slows down because of the presence of impurities and structural defects, which in turn limit the doping level and results in the trapping of the charge carriers [82, 83]. The increase in dc conductivity and mechanism of charge transport depend on the extent of doping level and formation and distribution of conducting domains within the polymer matrix (figures 4(c)–(f)) [60], [84]–[87].

In general, the dc conductivity (σ_{dc}) of conjugated polymers can be assumed [60, 88] to consist of three components, σ_B, σ_H and σ_T, i.e.

$$\sigma_{dc} = \sigma_B + \sigma_H + \sigma_T, \tag{1}$$

where σ_B is conductivity due to intra-chain transport of charge carriers which can be described by the band conduction mechanism and is usually observed at high temperatures. σ_H is the contribution to the total conductivity (σ_{dc}) due to inter-chain transport of charge carriers, i.e. hopping of charge carriers between the polymer chains and is observed at intermediate temperature or below room temperature. σ_T is the conductivity usually observed at low temperature and is due to thermally activated tunnelling. Earlier Mott [89] visualized such a situation in terms of the movement of electronic charge carriers. Each time an electron moves between the polymer chains, an electron just below the Fermi level jumps normally to a state just above it with energy W and transfers from one chain to the adjacent chain of which the wavefunction overlaps that of the first chain. Hence in the present investigation the total observed dc conductivity (σ_{dc}) of P3HT films may be correlated with the conductivity σ_H for the hopping of charge carriers between the chains from room temperature down to 40 K and below it the conductivity is associated with the tunnelling conduction [59, 60, 90]. Thus the electrical transport between the chains (inter-chain transport) in P3HT films is easier than the intra-chain transport, as was observed earlier in case of polypyrrole films [88].

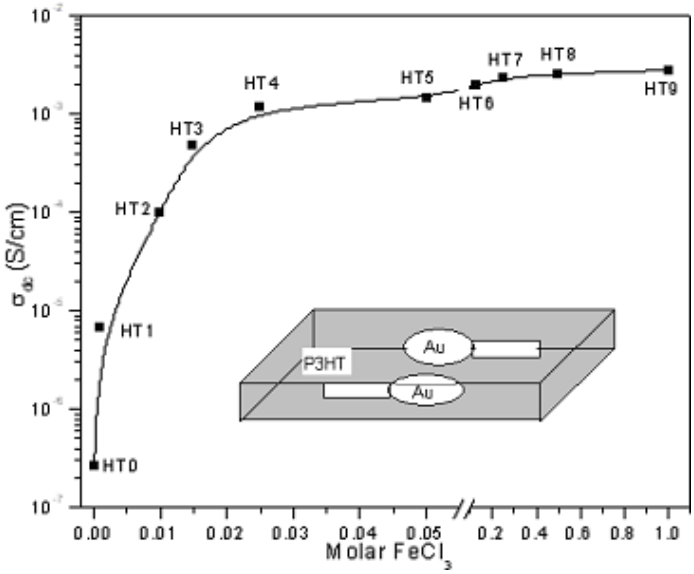

Figure 5. Plot of dc conductivity as a function of $FeCl_3$ molar concentration. The inset shows the geometrical representation of the sample in Au/P3HT/Au sandwiched structure used for dc conductivity measurement.

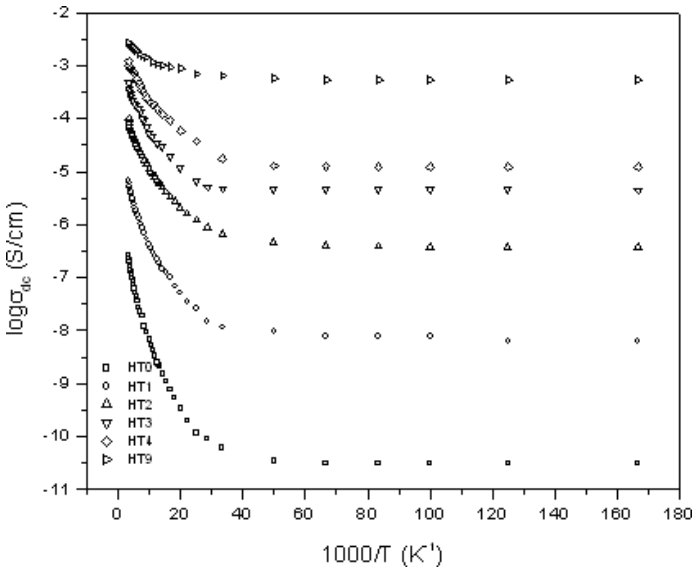

Figure 6. The plot of dc conductivity (σ_{dc}) as a function of reciprocal temperature in the range 6–300 K.

3.6. Temperature dependence of dc conductivity

Figure 6 shows the variation of dc conductivity (σ_{dc}) as a function of reciprocal temperature in the range 6–300 K for P3OT samples having different dopant concentrations. It is evident from this figure that the dc conductivity tends to saturate in the low temperature region. The temperature at which the saturation starts is higher for higher dopant concentration.

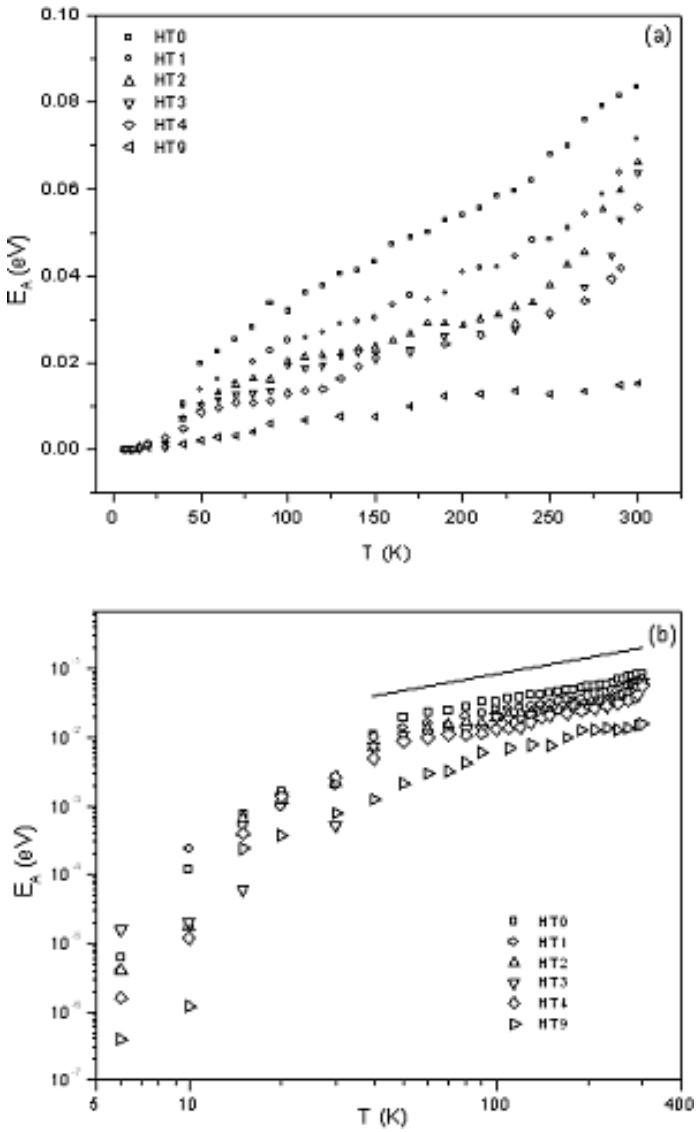

Figure 7. Plot of (a) E_A versus T and (b) log E_A versus log T in the temperature range 6–300 K. The solid line corresponds to $T^{-1/4}$, slope $m = 1/4$.

The activation energy evaluated from figure 6 is plotted as a function of temperature in figure 7(a). The temperature-dependent activation energy [39] reveals that the band conduction model will not be able to explain the temperature-dependence of dc conductivity (figure 6) of pristine and doped P3HT films. Then some other possibilities could be thought of, which may govern the charge transport in P3HT films. One possibility is the temperature-dependent band gap or energy gap E_g. In such a situation, the activation energy E_A can be defined [55] as

$$E_A = \left\{ \frac{-\partial \ln \sigma}{\partial (1/k_B T)} \right\}, \tag{2}$$

where k_B is Boltzmann's constant. We write the expression for dc conductivity as

$$\sigma_{dc} = \sigma_0' \exp\left\{\frac{-(E_C - E_F)}{k_B T}\right\}, \tag{3}$$

where σ_0' is a pre-exponential factor. If we assume that the distance of the Fermi energy E_F from the conduction band edge E_C, i.e. $(E_C - E_F)$, is temperature dependent, then E_A can be written as

$$E_A = (E_C - E_F) - T\left\{\frac{\partial}{\partial T}(E_C - E_F)\right\}. \tag{4}$$

If the energy gap Eg is considered to be temperature dependent, then E_A will become

$$E_A = E_g - T(\partial E_g/\partial T) - (E_F - E_V). \tag{5}$$

The term $(E_F - E_V)$ in equation (5) is assumed to be temperature independent. This indicates that the temperature dependence of the energy gap has to be supralinear in order to account for the temperature dependence of activation energy (figure 7(a)). It is evident from figure 7(a) that E_A increases almost linearly with temperature and it cannot be explained by assuming a temperature-dependent band gap or energy gap. Hence, the failure of a simple band conduction model in explaining the temperature dependence of conductivity indicates that the hopping transport dominates the mechanism of charge transport in P3HT films.

Then the dc conductivity data of the present investigation was first examined by Kivelson's model [32] in which the inter-chain transport occurs by hopping between neutral and charged soliton states at iso-energetic levels. The neutral solitons are mobile along the carbon chain whereas the charged solitons are pinned next to the dopant ions and their roles are inter-chained in the hopping process. The temperature dependence of dc conductivity in such a situation can be approximated by a simple power law given [32] as

$$\sigma = AT^n, \tag{6}$$

where A is a constant and the power index 'n' typically lies around ten or above. This model was modified for the case of inter-polaronic hopping conduction in conjugated polymers having a non-degenerate ground state wherein the hopping phenomenon takes place between a polaron and bipolaron both pinned by counter ions [46]. The measured dc conductivity data of the present work (temperature range 6–300 K) has been plotted as $\log \sigma_{dc}$ versus $\log T$ for pristine and different doped samples of P3HT in figure 8. It is evident from this figure that the simple power law given in equation (6) is not satisfied in the present investigation and the value of 'n' lies in the range ~0.65 to 3.73 indicating thereby its deviation from Kivelson's model [32]. The electron spin resonance (ESR) line shape for P3HT samples is of Lorentzian type and almost symmetric, i.e. A/B ratio is ~1, which indicates that the probability of oxygen attack on the samples is very small. A single Lorentzian ESR line shape observed for P3HT films rules out the formation of metallic islands [89]. Henceforth, the temperature variation of dc conductivity has been analysed in terms of Mott's VRH model [55] in which the dc conductivity is of the form

$$\sigma_H = \sigma_0 \exp\left\{-\left(\frac{T_0}{T}\right)^m\right\}, \tag{7}$$

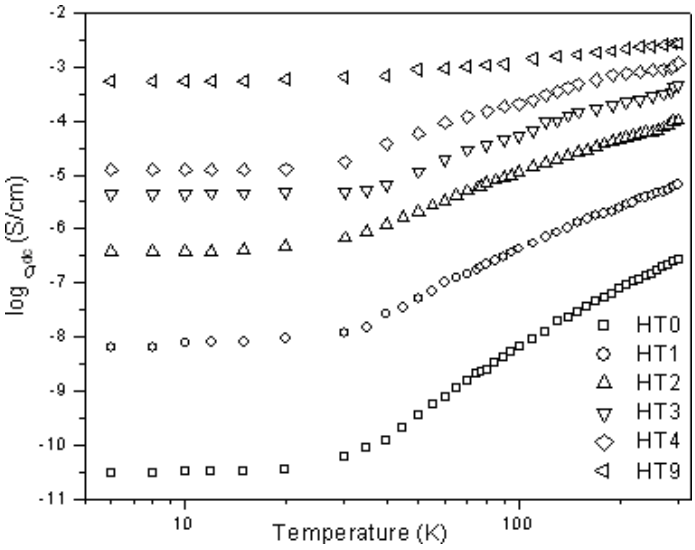

Figure 8. The plot of log of dc conductivity (σ_{dc}) as a function of log of temperature in the range 6–300 K.

where σ_0 and T_0 are constants. T is the temperature and $m = 1/d + 1$, where d is the dimensionality. A plot of log σ_H versus $(1/T)^m$ should give a straight line for proper value of m. It is seen from figure 6 that the conductivity data do not fit the straight line for the entire temperature range. It tends to saturate below ∼40 K for all the samples. Figure 6 shows the applicability of the 3D-VRH model above 40 K which indicates that the charge transport occurs by phonon-assisted hopping which are thermally activated jumps between the localized sites. At low temperatures below 40 K, the conductivity becomes less activated and the mechanism of charge transport can be attributed to the tunnelling mechanism reported earlier for other conjugated polymers [59, 60, 91]. In the present investigation (figure 6), two distinct mechanisms of charge transport dominate, one in the lower (below 40 K) and other in the higher (40–300 K) temperature region.

Therefore, the dc conductivity data in the temperature range 40–300 K has been examined in terms of Mott's VRH model [55]. For this, the dc conductivity data of all the samples were plotted as functions of $T^{-1/2}$ and $T^{-1/4}$ in the temperature range 40–300 K in figures 9(a) and (b). The linearity factor of $T^{-1/2}$ and $T^{-1/4}$ plots are given in table 2. It is seen from table 2 that the linearity factor for $T^{-1/4}$ gives the best fit for pristine P3HT and then for doped samples, it starts decreasing and finally for sample HT9 the linearity factor is better in case of $T^{-1/2}$ rather than $T^{-1/4}$. The plots (figure 9(b)) in the temperature region (40–300 K), where equation (9) is valid should give an activation energy as equation (2) and can be correlated to the parameters of equation (7) by the following expression

$$E_A = mk_B T_0 \, (T_0/T)^{m-1} \, . \tag{8}$$

It is evident from equation (8) that a plot of log E_A versus log T should yield a straight line of slope $-(m - 1)$. The plot of log of activation energy (evaluated from figure 6) as a function of log T is given in figure 7(b). It can be seen from this figure that the activation energy shows a systematic decrease with decreasing temperature. A straight line corresponding to $m = 1/4$ is also shown in figure 7(b). It appears that the value of $m = 1/4$ may satisfy the variation of

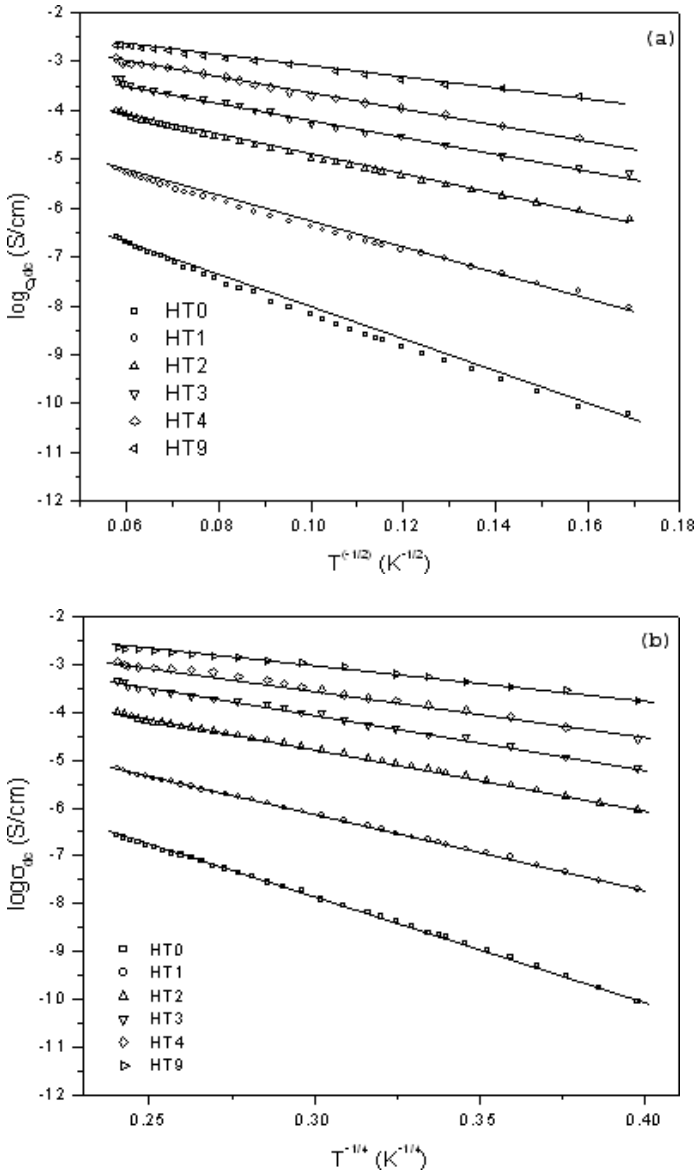

Figure 9. The hopping conductivity (σ_H) plotted as functions of (a) $T^{-1/2}$ and (b) $T^{-1/4}$ in the temperature range 40–300 K.

activation energy with temperature. This indicates that the VRH mechanism of type $T^{-1/4}$ which may dominate the mechanism of conduction in pristine and lightly doped P3HT films in the temperature range 40–300 K [39].

Equations (7) and (8) give the slope T_0 [39, 40, 60, 88] of the plots of log σ_{dc} versus $T^{-1/4}$ (figure 9(b)) as

$$T_0 = \frac{B_0 \alpha^3}{k_B N\,(E_F)} \tag{9}$$

Table 2. Values of conductivity (σ_{dc}) and Mott's parameters: linearity factor, dc conductivity (σ_{dc}), characteristic temperature (T_0), density of states at the Fermi level ($N(E_F)$), average hopping distance (R), average hopping energy (W) for pristine and doped P3HT films.

Sample no.	Linearity factor $T^{-1/2}$	Linearity factor $T^{-1/4}$	σ_{dc} (S cm^{-1})	T_0 (K)	$N(E_F)$ (cm^{-3} eV^{-1})	R (Å)	R (eV)	W αR
HT0	0.99254	0.99936	2.61×10^{-7}	5.61×10^{6}	1.06×10^{20}	25.4	0.137	7.97
HT1	0.99839	0.99930	6.61×10^{-6}	1.82×10^{6}	3.27×10^{20}	19.2	0.104	6.02
HT2	0.99860	0.99932	1.01×10^{-5}	7.13×10^{5}	8.36×10^{20}	15.2	0.082	4.77
HT3	0.99575	0.99808	4.69×10^{-4}	4.54×10^{5}	1.31×10^{21}	13.5	0.071	4.24
HT4	0.99744	0.99621	1.18×10^{-3}	3.61×10^{5}	1.65×10^{21}	12.8	0.069	4.02
HT9	0.99899	0.99782	2.76×10^{-3}	7.47×10^{4}	7.97×10^{21}	8.6	0.047	2.70

where T_0 is the characteristic temperature. B_0 is the dimensionless constant and is assumed to be ~1.66 [40, 55], k_B is Boltzmann's constant, $N(E_F)$ is the density of states at the Fermi level and $\alpha(=1/r_p)$ is the coefficient of exponential decay of the localized states involved in the hopping process. The accurate estimation of T_0 from figure 9(b) gives the estimation of $N(E_F)$, i.e. the density of states at the Fermi level, which in turn provides the estimation of average hopping distance R and average hopping energy W. The other constant σ_0 in equation (7) is given by

$$\sigma_0 = e^2 R^2 \nu_{ph} N(EF), \tag{10}$$

where

$$R = \left\{ \frac{9}{8\pi\alpha k_B T N(E_F)} \right\}^{1/4}, \tag{11}$$

is the average hopping distance between the two sites. ν_{ph} is a phonon frequency (~10^{13} Hz) and can be obtained from Debye temperature θ_D. The average hopping energy W can be estimated by knowing the average hopping distance R and the density of states at the Fermi level $N(E_F)$ by the following relation

$$W = \frac{3}{4\pi R^3 N(E_F)}. \tag{12}$$

The values of various Mott's parameters T_0, $N(E_F)$, R, W for all the samples of P3HT films have been evaluated by using equations (9)–(12) and are given in table 2. In these calculations, it has been assumed [39, 40, 60, 92] that the electron wavefunction localization length, i.e. $\alpha^{-1}(r_p)$ is equal to the width of the thiophene monomer unit, i.e. ~3.185 Å [93], since the electrons are always at least delocalized to the extent of the π-orbitals on the monomer units [40]. This parameter yields the density of states at the Fermi level; ($N(E_F)$) on the assumption that the wavefunction localization length remains independent of temperature and conductivity. The values of T_0 has been estimated from the slope of $\log \sigma_{dc}$ versus $T^{-1/4}$ (figure 9(b)) and

found to decrease with increase in the sample conductivity. Similarly R and W for all samples have been evaluated by using equations (11) and (12). The values of T_0, R, W and $N(E_F)$ are given in table 2. It can be seen from table 2 that the density of states at the Fermi level; $N(E_F)$ of pristine and doped P3HT films lies in the range of 10^{20}–10^{21} cm^{-3} eV^{-1} which is in good agreement with the values reported earlier for other polyheterocyclics [39, 40, 56, 57, 59, 60] and several other conjugated polymeric systems [37, 44, 46, 91, 94]. Our results are consistent with the Mott's requirement that $\alpha R \gg 1$ and $W \gg k_B T$ for conductivity by hopping to distant sites. The temperature-dependent activation energy (figure 7(a)) and evaluated values of Mott's parameters (table 2) suggest that the Mott's 3D-VRH model successfully explains the mechanism of charge transport in pristine and lightly doped P3HT films in the temperature range 40–300 K.

4. Conclusions

In conclusion, P3HT has been chemically doped by varying concentration of $FeCl_3$. FT-IR and UV–Vis spectra reveal the formation of P3HT–$FeCl_3$ charge-transfer complexes. XRD studies shows physical approach of dopant molecules to P3HT π-conjugated chains required for exchange of electrons between the two. AFM studies supplement the formation of charge-transfer complexes in terms of discrete conducting domains, which not only control the increase in conductivity but also determine the mode of charge transport. The measured dc conductivity data of pristine P3HT and P3HT–$FeCl_3$ charge-transfer complexes in the temperature range 40–300 K is predominantly governed by Mott's 3D-VRH; however, below 40 K tunnelling seems to dominate. A slight deviation is observed (table 2) in the linearity factor of $T^{-1/4}$ (3D-VRH) and $T^{-1/2}$ (1D-VRH) with increase in doping level. We attribute this deviation to the induced expansion in crystallographic lattices due to insertion and intercalation of dopant species in between π–π stacks and to the formation of discrete conducting domains separated by undoped regions of polymer matrices.

Acknowledgments

We thank Dr S Mazumdar, Department of Chemistry, University of Delhi, and to Drs S T Lakshmikumar, M N Kamalasanan, S K Halder, S K Dhawan, and H K Singh, National Physical Laboratory, New Delhi for their cooperation and useful discussion. RKS thanks the Ministry of Non-Conventional Energy Sources (MNES), Government of India, New Delhi for the award of a Junior Research Fellowship.

References

[1] Chiang C K, Druy M A, Gau S C, Heeger A J, Louis E J, MacDiarmid A G, Park Y W and Shirakawa H 1978 *J. Am. Chem. Soc.* **100** 1013

[2] Chiang C K, Park Y W, Heeger A J, Shirakawa H, Louis E J and MacDiarmid A G 1978 *J. Chem. Phys.* **69** 5098

[3] Guiseppi-Elie A, Wallace G G and Matsue T 1998 *Handbook of Conducting Polymers* 2nd edn (New York: Dekker)

[4] Zotti G 1997 *Handbook of Conductive Molecules and Polymers* vol 2 (Chichester: Wiley)
[5] Friend R C and Greenham N C 1998 *Handbook of Conducting Polymers* 2nd edn (New York: Dekker)
[6] Saoudi B, Jammul N, Abel M-L, Chehimi M M and Ddin G 1997 *Syn. Met.* **87** 97
[7] Arbizzani C, Gastragostine M and Scrosati B 1997 *Handbook of Conductive Molecules and Polymers* vol 2 (Chichester: Wiley)
[8] Sirringhaus H, Tesler N and Friend R H 1998 *Science* **280** 1741
[9] Dodabalapur A, Bao Z, Makhija A, Laquindanum J G, Raju V R, Feng Y, Katz H E and Rogers J 1998 *Appl. Phys. Lett.* **73** 142
[10] Liu J, Kadnikova E N, Liu Y, McGehee M D and Frechet J M J 2004 *J. Am. Chem. Soc.* **126** 9486
[11] Zhang H, Boussaad S, Ly N and Tao N J 2004 *Appl. Phys. Lett.* **84** 133
[12] Sun S, Anders S, Hamann H F, Thiele J-U, Baglin J E E, Thomson T, Fullerton E E, Murray C B and Terris B D 2002 *J. Am. Chem. Soc.* **124** 2884
[13] Shaheen S E, Brabec C J, Sariciftci N S, Padinger F, Fromherz T and Hummelen J C 2001 *Appl. Phys. Lett.* **78** 841
[14] Drury C J, Mutsaers C M J, Hart C M, Matters M and de Leeuw D M 1998 *Appl. Phys. Lett.* **73** 108
[15] Ong B S, Wu Y, Liu P and Gardner S 2004 *J. Am. Chem. Soc.* **26** 3378
[16] Poplavskyy D, Nelson J and Bradley D D C 2003 *Appl. Phys. Lett.* **83** 707
[17] Kaeriyama K 1997 *Handbook of Organic Conductive Molecules and Polymers* vol 2, ed H S Nalwa (Chichester: Wiley)
[18] Keibooms R, Menon R and Lee K 2001 *Handbook of Advanced Electronic and Photonic Materials and Devices* vol 8 (New York: Academic)
[19] Bredas J L 1986 *Handbook of Conducting Polymers* vol 2 (New York: Dekker)
[20] Nalwa H S 1989 *Phys. Rev.* B **39** 5964
[21] Houze E and Nechtschein M 1996 *Phys. Rev* B **53** 14309
[22] Scott J C, Pfluger P, Krounbi M T and Street G B 1983 *Phys. Rev.* B **28** 2140
[23] Pereira E C, Bulhoes L O, Pawlika A, Nascimento O R, Faria R M and Walmstag L 1994 *Phys. Rev.* B **50** 3648
[24] Mizoguchi K, Honda M, Kachi N, Shimizu F, Sakamoto H, Kume K, Masubuchi S and Kazama S 1995 *Solid State Commun.* **96** 333
[25] Genoud F, Guglielmi M, Nechtschein M, Geneis E and Salmon M 1986 *Phys. Rev. Lett.* **55** 118
[26] Devreux F 1986 *Europhys. Lett.* **1** 233
[27] Bacsai J, Inzlet G, Bartl A, Dunsch L and Pasch G 1994 *Synth. Met.* **67** 227
[28] Nechtschein M, Devreux F, Genoud F, Viell E, Pernaut J M and Geneis E 1986 *Synth. Met.* **15** 59
[29] Kaufman J H, Colaneri N, Scott J and Street G B 1984 *Phys. Rev. Lett.* **53** 1005
[30] Bloor D and Movaghar B 1983 *IEE Proc.* **130** 225
[31] Su W P, Schrieffer J R and Heeger A J 1981 *Phys. Rev.* B **22** 2099
[32] Kivelson S 1981 *Phys. Rev. Lett.* **46** 1344
Kivelson S 1982 *Phys. Rev.* B **25** 3798
[33] Sun S, Chen L and Yu E X 1985 *Solid State Commun.* **53** 973
[34] Singh R, Tandon R P, Singh G S and Chandra S 1992 *Phil. Mag.* B **66** 285
[35] Lee K, Menon R, Yoon C O and Heeger A J 1995 *Phys. Rev.* B **52** 4779
[36] Reghu M, Subramanium S V and Chatterjee S 1991 *Phys. Rev.* B **43** 4236
[37] Zuo F, Angelopoulos M, MacDiarmid A G and Epstein A J 1989 *Phys. Rev.* B **39** 3570
[38] Zuppiroli L, Bussac M N, Paschen S, Chauvet O and Forro L 1994 *Phys. Rev.* B **50** 5196
[39] Singh R, Narula A K, Tandon R P, Mansingh A and Chandra S 1996 *J. Appl. Phys.* **79** 1476
[40] Maddison D S and Tansley T L 1992 *J. Appl. Phys.* **72** 4677
[41] Kaiser A B 1989 *Phys. Rev.* B **40** 2806
[42] Sheng P and Klafter J 1983 *Phys. Rev.* B **27** 2583
[43] Punka E, Rubner M F, Hettinger J D, Brooks J S and Hannahs S T 1991 *Phys. Rev.* B **43** 9076

[44] Rouleau J F, Goyette J, Bose T K, Singh R and Tandon R P 1995 *Phys. Rev.* B **52** 4801
[45] Epstein A J, Rommelmann H, Bigelow R, Gibson H W, Hoffman D and Tanner D B 1983 *Phys. Rev. Lett.* **50** 1866
Epstein A J, Rommelmann H, Bigelow R, Gibson H W, Hoffman D and Tanner D B 1983 *Phys. Rev. Lett.* **51** 2020
[46] Kuivalainen P, Stubb H, Isotalo M, Yli-Lahti P and Holmstrom C 1971 *Phys. Rev.* B **4** 2612
[47] Singh R, Narula A K, Tandon R P, Mansingh A and Chandra S 1996 *J. Appl. Phys.* **80** 985
[48] Pinto N J, Torres C M, Kahol P K and McCormick B J 1996 *J. Appl. Phys.* **79** 8512
[49] Audenaert M 1984 *Phys. Rev.* B **30** 4609
[50] Valaski R, Moreira L M, Micaroni L and Hummelgen I A 2003 *Braz. J. Phys.* **33** 392
[51] Paasch G, Lindner T and Scheinert S 2002 *Synth. Met.* **132** 97
[52] Prigodin V N, Samukhin A N and Epstein A J 2004 *Synth. Met.* **141** 155
[53] Dicker G, de Haas M P, Siebbeles D A and Warman J M 2004 *Phys. Rev.* B **70** 045203
[54] Kapoor A K, Jain S C, Poortmans J, Kumar V and Mertens R 2002 *J. Appl. Phys.* **92** 3835
[55] Mott N F and Davis E A 1979 *Electronic Processes in Noncrystalline Materials* 2nd edn (London: Oxford University Press)
[56] Singh R, Narula A K, Tandon R P, Mansingh A and Chandra S 1997 *J. Appl. Phys.* **81** 3726
[57] Singh R and Narula A K 1997 *J. Appl. Phys.* **82** 4362
[58] Spatz J P, Loarentz B, Weishopt K, Hochheimer H D, Menn V, Parthasarthy R, Martine R, Bechtold C R and Hor P H 1992 *Phys. Rev.* B **50** 343
[59] Singh R, Kaur A, Yadav K L and Bhattacharya D 2003 *Curr. Appl. Phys.* **3** 235
[60] Kumar J, Singh R K, Chand S, Kumar V, Rastogi R C and Singh R 2006 *J. Phys. D: Appl. Phys.* **39** 196
[61] Yang C Y, Soci C, Moses D and Heeger A J 2005 *Synth. Met.* **155** 639
Kaniowski T, Luzny W, Niziol S, Sanetra J and Trznadel M 1998 *Synth. Met.* **92** 7
[62] Genevicius K, Osterbacka R, Juska G, Arlauskas K and Stubb H 2002 *Thin Solid Films* **403–404** 489
[63] Mardalen J, Samuelsen E J, Konestabo O R, Hanfland M and Lorenzen M 1998 *J. Phys.: Condens. Matter* **10** 7145
[64] Konestabo O R, Aasmundtveit K E, Samuelsen E J, Bakken E and Carlsen P H J 1997 *Synth. Met.* **84** 589
[65] Luzny W, Trznadel M and Porn A 1996 *Synth. Met.* **81** 71
[66] Fell H J, Samuelsen E J, Andersson M R, Als-Nielsen J, Gruebel G and Mardalen J 1995 *Synth. Met.* **73** 279
[67] Mardalen J, Cerenius Y and Haggkvist P 1995 *J. Phys.: Condens. Matter* **7** 3501
[68] Fell H J, Samuelsen E J, Als-Nielsen J, Gruebel G and Mardalen J 1995 *Solid State Commun.* **94** 843
[69] Prosa T J, Winokur M J, Moulton J, Smith P and Heeger A J 1995 *Phys. Rev.* B **51** 159
[70] Kaniowski T, Niziol S, Sanetra J, Trznadel M and Porn A 1998 *Synth. Met.* **94** 111
[71] Liu Y Q, Jiang X Z, Li Q L, Xu Y and Zhu D B 1997 *Synth. Met.* **85** 285
[72] Park B K, Park D H, Kook S H and Yoshino K 1991 *Trans. Korean Inst. Electr. Eng.* **40** 91
[73] Gustafsson G, Inganas O and Stafstrom S 1990 *Solid State Commun.* **76** 203
[74] Ong B S, Wu Y, Liu P and Gardner S 2005 *Adv. Mater.* **17** 1141
[75] Gao Z, Siow K S and Chan H S O 1995 *Synth. Met.* **75** 5
[76] Chen T-A, Wu X and Rieke R D 1995 *J. Am. Chem. Soc.* **117** 233
[77] Youm I, Cadene M and Lapeze D 1995 *J. Mater. Sci. Lett.* **14** 1712
[78] Singh R, Kumar J, Singh R K, Kaur A, Sood K N and Rastogi R C 2005 *Polymer* **46** 9126
[79] Amou S, Haba O, Shirato K, hayakawa T, Ueda M, Takeuchi K and Asai M 1999 *J. Polym. Sci. A: Polym. Chem.* **37** 1943
[80] Andersson M R, Selse D, Berggren M, Järvinen H, Hjertberg T, Inganass O, Wennerstoerm O and Oesterholm J E 1994 *Macromolecules* **27** 650
[81] Sandberg M, Tanaka S and Kaeriyama K 1993 *Synth. Met.* **57** 3587
[82] Tourillon G 1986 *Handbook of Conducting Polymers* vol 1 (New York: Dekker)
[83] Yamamoto T, Sanechika K and Yamamoto A 1983 *Bull. Chem. Soc. Japan* **56** 1503

[84] Wu C-G and Chang S S 2005 *J. Phys. Chem.* B **109** 825
[85] Tourillon G and Garnier F 1983 *J. Phys. Chem.* **87** 2289
[86] Tourillon G and Garnier F 1984 *J. Polym. Sci. Polym. Phys. Edn.* **22** 33
[87] Narula A K, Singh R, Yadav K L, Ravat K B and Chandra S 2001 *Appl. Biochem. Biotech.* **96** 109
[88] Singh R, Tandon R P and Chandra S 1991 *J. Appl. Phys.* **70** 243
[89] Mott N F 1974 *Metal Insulator Transitions* (London: Taylor and Francis)
[90] Moraes P, Chen J, Chung T-C and Heeger A J 1985 *Synth. Met.* **11** 271
[91] Reghu M and Subramanyam S V 1989 *Solid State Commun.* **72** 325
[92] Paul D K and Mitra S S 1973 *Phys. Rev. Lett.* **31** 1000
[93] Samuelsen E J and Mardalen J 1997 *Handbook of Organic Conductive Molecules and Polymers* vol 3, ed H S Nalwa (Chichester: Wiley) p 87
[94] Meikap A K, Das A, Chatterjee S, Digar M and Bhattacharya S N 1993 *Phys. Rev.* B **47** 134